Continuum wave functions for estimating the electric dipole moment: Calculation based on a multiconfiguration Dirac-Hartree-Fock approximation

Paweł Syty[*] and Józef E. Sienkiewicz

Faculty of Applied Physics and Mathematics, Gdańsk University of Technology, Narutowicza 11/12, 80-233 Gdańsk, Poland

Laima Radžiūtė, Gediminas Gaigalas, and Pavel Rynkun

Institute of Theoretical Physics and Astronomy, Vilnius University, Saulėtekio Avenue 3, 10222 Vilnius, Lithuania

Jacek Bieroń

Marian Smoluchowski Institute of Physics, Jagiellonian University, Łojasiewicza 11, 30-348 Kraków, Poland

The multiconfiguration Dirac-Hartree-Fock method is employed to calculate the continuum electron wave functions, which are then used to estimate their contribution to the atomic electric dipole moment (EDM) of ^{129}Xe. The EDM arises from (P, T)-odd electron-nucleon tensor-pseudotensor and pseudoscalar-scalar interactions, the nuclear Schiff moment, the interaction of the electron electric dipole moment with nuclear magnetic moments, and atomic electric dipole matrix elements. In addition to being estimated in the continuum states, all of these interactions are also estimated in the ground state, as well as in the Rydberg states of ^{129}Xe. Calculations of one-electron atomic orbitals include the interelectronic interactions, through valence and core-valence electron correlation effects. The contribution to the EDM from continuum states is found to be of the same order of magnitude as the contribution from discrete states.

I. INTRODUCTION

In recent years the electric dipole moments (EDMs) of elementary particles, nuclei, atoms, and molecules have been the subject of intensive experimental and theoretical studies. The importance of these studies arises from the fact that the discovery of a nonzero permanent EDM of an elementary particle, or in a nondegenerate system of particles, would constitute a proof of violation of parity P and time-reversal T symmetries [1,2].

The experimental searches have not yet detected a nonzero EDM, but they continue to improve the limits on EDMs of individual elementary particles, as well as limits on CP-violating interactions [1,3,4]. Nowadays, the focus is on an EDM of diamagnetic atoms like Xe or Hg. The combined statistical and systematic errors in the case of ^{129}Xe are by two order of magnitude higher than in the case of ^{199}Hg [5]. Despite this, the measurements of the Xe EDM have significant potential for improvements in the experimental limit by using a nuclear spin maser technique [6,7]. Recent experimental studies on the ^{129}Xe and ^{3}He mixture in a newly designed EDM cell indicate the possibility of improving the EDM upper limit by at least of one order of magnitude to achieve the accuracy as low as 10^{-28} e cm [8], while the most precise measurement of the EDM induced in ^{129}Xe gives the value of [9] $d(^{129}$Xe$) = (0.7 \pm 3.3 \pm 0.1) \times 10^{-27}$ e cm.

Some diamagnetic atoms, including noble gases like Xe and Rn, have been investigated within the Hartree-Fock approximation in the V^N self-consistent potential formed from all N electrons [10]. In turn, calculations based on the relativistic-coupled-cluster theory in combination with the measurement of the EDM of a ^{129}Xe atom gave the parity and time-reversal odd coupling constant associated with the tensor-pseudotensor electron-nucleus interaction and the nuclear Schiff moment [11].

When using the multiconfiguration Dirac-Hartree-Fock (MCDHF) approximation it is important to understand the importance of continuum states for calculation of the EDM, because we expect that the contribution of continuum states can be different for many-body perturbation theory (MBPT) and MCDHF approximations. There are several papers on EDM calculations in which different approximations were used and bound states summations were done explicitly, but the contribution from continuum states was not singled out [12,13]. Only in the rather special case of the ground state of hydrogen [14], the contribution of continuum states was calculated explicitly and accounted for 53%.

The main goal of this paper is to demonstrate the method for generation of continuum state functions for EDM application in the MCDHF approximation. As an example, the contribution of the continuum states for the EDM was calculated and compared to the contributions from discrete states in the ground state of ^{129}Xe, as well as from the Rydberg states. To ensure the correctness of our approach, we obtained detailed insight into the behavior of the electron wave function while passing through the ionization energy. Let us stress that this is a numerically obtained estimation of the contribution of the continuum states to the atomic EDM.

---
[*]pawel.syty@pg.edu.pl

Discrete states were calculated with the relativistic atomic structure package GRASP2K [15], based on the MCDHF approach. Continuum states were calculated using the COWF code [16] prepared in frames of the RATIP package [17], adapted to GRASP2K. Time and parity (P, T)-odd electron-nucleon tensor-pseudotensor (TPT) and pseudoscalar-scalar (PSS) interactions, the nuclear Schiff moment (NSM), interaction of the electron electric dipole moment (eEDM) with nuclear magnetic moments operators, and expressions of matrix elements are presented in [18].

II. GENERAL THEORY OF THE BOUND STATE

We have used the MCDHF approach to generate numerical representations of atomic wave functions. An atomic-state function (ASF) $\Psi(\gamma P J M_J)$ was obtained as a linear combination of configuration-state functions $\Phi(\gamma_r P J M_J)$, eigenfunctions of the parity P, total angular momentum operators J^2, and the projection M_J,

$$\Psi(\gamma P J M_J) = \sum_r c_r \Phi(\gamma_r P J M_J), \tag{1}$$

where c_r are configuration mixing coefficients. The multiconfiguration energy functional is based on the Dirac-Coulomb Hamiltonian, given (in a.u.) by

$$\hat{H}_{DC} = \sum_{j=1}^N [c\boldsymbol{\alpha}_j \cdot \boldsymbol{p}_j + (\beta_j - 1)c^2 + V(r_j)] + \sum_{j<k}^N \frac{1}{r_{jk}}, \tag{2}$$

where $\boldsymbol{\alpha}$ and β are the Dirac matrices and $\boldsymbol{p}$ is the momentum operator. The sum runs over a number of electrons N. The electrostatic electron-nucleus interaction $V(r_j)$ was generated from a two-parameter Fermi nuclear charge distribution. The effects of the Breit interaction as well as QED effects were neglected since they are expected to be small at the level of accuracy attainable in the present calculations.

The atomic-state functions (1) were obtained as expansions over jj-coupled configuration-state functions (CSFs). To provide the LSJ labeling system, the ASFs were transformed from a jj-coupled CSF basis into an LSJ-coupled CSF basis using the method provided by [19,20].

III. GENERAL THEORY OF THE CONTINUUM STATE

In the MCDHF approach, we express the total wave function of the N-electron ^{129}Xe system with one electron in the continuum in the form [21]

$$\Psi(\gamma P J M_J; N) = \Psi^{ion}(\gamma P J M_J; N - 1) u_{\kappa m}. \tag{3}$$

The right-hand side of Eq. (3) is the product of the bound configuration states of the ion and the one-electron continuum spinor $u_{\kappa m}$. Let us stress that the ionic bound states were constructed from the atomic ones according to (1), by removing one of the bound electron.

The continuum Dirac spinor is defined as

$$u_{\kappa m}(\mathbf{r}) = \frac{1}{r} \begin{pmatrix} P_{\kappa\epsilon}(r) \chi_{\kappa m}(\mathbf{r}/r) \\ i Q_{\kappa\epsilon}(r) \chi_{-\kappa m}(\mathbf{r}/r) \end{pmatrix}, \tag{4}$$

where $P_{\kappa\epsilon}$ and $Q_{\kappa\epsilon}$ refer to continuum orbitals and the spin-angular function is given by

$$\chi_{\kappa m}(\mathbf{r}/r) = \sum_{\sigma=\pm 1/2} \langle jm | l, \tfrac{1}{2}, m - \sigma, \sigma \rangle Y_l^{m-\sigma}(\mathbf{r}/r) \chi_{1/2}^\sigma, \tag{5}$$

where $\langle jm | l, \tfrac{1}{2}, m - \sigma, \sigma \rangle$ is a Clebsch-Gordan coefficient, $Y_l^{m-\sigma}(\mathbf{r}/r)$ is a spherical harmonic, $\chi_{1/2}^\sigma$ is the spin eigenfunction, κ is the relativistic angular quantum number, with $\kappa = \pm(j + 1/2)$ for $l = j \pm 1/2$, where j is the total angular momentum and l and m are the orbital and magnetic quantum numbers, respectively. These continuum orbitals are solutions of the Dirac-Fock (DF) equations

$$\left(\frac{d}{dr} + \frac{\kappa}{r}\right) P_{\kappa\epsilon}(r) - \left(2c - \frac{\epsilon}{c} + \frac{V(r)}{cr}\right) Q_{\kappa\epsilon}(r) = -\frac{X^{(P)}(r)}{r},$$
$$\left(\frac{d}{dr} - \frac{\kappa}{r}\right) Q_{\kappa\epsilon}(r) + \left(-\frac{\epsilon}{c} + \frac{V(r)}{cr}\right) P_{\kappa\epsilon}(r) = \frac{X^{(Q)}(r)}{r}. \tag{6}$$

Here ϵ is the kinetic (positive) energy of the continuum electron. Direct $V(r)$ and exchange $X(r)$ potentials are given in [22]. These equations were solved by the method of outward integration to obtain the (radial) continuum wave functions $P_{\kappa\epsilon}$ and $Q_{\kappa\epsilon}$. See [23,24] for a detailed description of the total wave function of the atom- (ion-) electron system and the method of solving Eq. (6).

The continuum wave function was normalized per unit energy [25], which means that the amplitude of the continuum spinor $P_{\kappa\epsilon}$ was adjusted to $2^{1/4}\pi^{-1/2}\epsilon^{-1/4}$. Then the small component $Q_{\kappa\epsilon}$ was also rescaled. Tests of normalization correctness are presented in Sec. VIII.

IV. THE EDM THEORY

The atomic EDM can be written as a sum consisting of two parts, the first for the bound states and the second for the electron in the continuum state (CS)

$$d_{at}^{int} = d_b^{int} + d_c^{int}, \tag{7}$$

where d_b^{int} represents the contribution to the atomic EDM from bound states and the d_c^{int} contribution from the electron in the continuum. These parts are detailed below. Like in Ref. [18], the EDM values of bound states were computed by the formula

$$d_b^{int} = 2 \sum_i \frac{\langle 0 | \hat{D}_z | i \rangle \langle i | \hat{H}_{int} | 0 \rangle}{E_0 - E_i}, \tag{8}$$

where $\hat{D}_z$ represents the z projection of the electric dipole moment operator, $|0\rangle$ represents the ground state $|\Psi(\gamma P J M_J)\rangle$, with $J = 0$ and even parity, and the summation runs over excited states $|\Psi(\gamma_i(-P)J_i M_{J_i})\rangle$, with $J_i = 1$ and odd parity. Here E_0 and E_i are the energies of the ground and excited states, respectively. In practice, this sum needs to be truncated at some level.

The second part is the contribution to the atomic EDM from the (P, T)-odd interactions between the electron in the continuum and bound electrons

$$d_c^{int} = 2 \int_0^\infty f^{int}(E_c) dE_c, \tag{9}$$

where

$$f^{\text{int}}(E_c) = \frac{\langle 0|\hat{D}_z|c\rangle\langle c|\hat{H}_{\text{int}}|0\rangle}{E_0 - E_c}. \quad (10)$$

According to Eq. (10), we need to calculate the matrix element between the ASF of the atom and the continuum electron wave function c of the total energy E_c, which in turn is the sum of the energy of the Xe^+ ion and kinetic energy ϵ of the electron. The ASF for the atom and ion is from the MCDHF and the wave function of the electron is from solving Eq. (6).

A Hamiltonian H_{int} consecutively becomes one of the interaction operators responsible for inducing the atomic EDM,

$$\hat{H}_{\text{TPT}} = i\sqrt{2}G_F C_T \sum_{j=1}^{N}((\langle \boldsymbol{\sigma}_A\rangle \cdot \boldsymbol{\gamma}_j)\rho(r_j)), \quad (11)$$

$$\hat{H}_{\text{PSS}} = \frac{-G_F C_P}{2\sqrt{2}m_p c}\sum_{j=1}^{N}\gamma_0(\boldsymbol{\nabla}_j\rho(r_j)\langle \boldsymbol{\sigma}_A\rangle), \quad (12)$$

$$\hat{H}_{\text{NSM}} = \frac{3}{B}\sum_{j=1}^{N}(\mathbf{S} \cdot \mathbf{r}_j)\rho(r_j), \quad (13)$$

$$\hat{H}_{\text{eEDM}} = -id_e\sum_{j=1}^{N}(\boldsymbol{\gamma}_j\mathbf{B}), \quad (14)$$

where G_F is the Fermi constant and C_T and C_P are dimensionless constants of TPT and PSS interactions, respectively. The Schiff moment $\mathbf{S}$ is directed along the nuclear spin I and $\mathbf{S} \equiv S\mathbf{I}/I$, where S is the coupling constant with units $|e|fm^3$, and d_e represents the electric dipole moment of the electron.

V. GENERATION OF BOUND-STATE WAVE FUNCTIONS

A. The Xe atom

Bound-state wave functions were generated in an extended optimal level (EOL) potential [26]. Wave functions for the ground state and for excited states were optimized separately in a nonorthogonal way. The atomic-state function expansions (1) were based on the active-space method.

TABLE I. The TPT (in $10^{-20}C_T\langle\sigma_N\rangle|e|$ cm), PSS (in $10^{-20}C_T\langle\sigma_A\rangle|e|$ cm), NSM (in $10^{-17}[S/(|e|\text{ fm}^3)]|e|$ cm), and eEDM (in $d_e \times 10^{-4}$) interaction contributions to the EDM, calculated with the EOL method in different virtual sets, for the ground state of ^{129}Xe. Here VOS enumerates the active sets; Th and Ex indicate the results obtained with excitation energy taken from GRASP2K and the NIST database [28], respectively.

	TPT		PSS		NSM		eEDM	
VOS	Th	Ex	Th	Ex	Th	Ex	Th	Ex
0 (DF)	0.16	0.15	0.44	0.43	0.12	0.11	0.10	0.11
1	0.18	0.20	0.51	0.59	0.12	0.14	0.16	0.19
2	0.17	0.34	0.47	0.97	0.10	0.19	0.27	0.61
3	0.16	0.35	0.47	1.00	0.10	0.20	0.26	0.59
4	0.15	0.32	0.43	0.92	0.09	0.19	0.22	0.51
5	0.16	0.33	0.45	0.95	0.09	0.20	0.24	0.54

TABLE II. The Xe^+ energies calculated with different virtual sets. The first column indicates the designation of the particular virtual set.

VOS	J	P	N_{CSF}	E (hartree)
0 (DF)	1/2		1	7436.32436840377
1	1/2		430	7436.43020217599
2	1/2		13080	7436.51799792548
3	1/2		53898	7436.53933399994
4	1/2		116350	7436.55170675590
0 (DF)	3/2		1	7436.37290018392
1	3/2		752	7436.47203134945
2	3/2		23248	7436.55470539355
3	3/2		96006	7436.57651624905
4	3/2		207122	7436.58950780784

Active space was generated by single and double (SD) excitations from valence shells ($5p$ and $6s$) and single restricted double (SRD) substitution from core shells of configurations $5p^6$ and $5p^56s$. Restricted double substitutions allow one excited electron from the core and another from the valence shells. The virtual orbital set (VOS) was restricted up to $l = g$ as follows:

$$\text{VOS}_1 = \{7s, 6p, 5d, 4f, 5g\},$$

$$\text{VOS}_2 = \text{VOS}_1 + \{8s, 7p, 6d, 5f, 6g\},$$

$$\text{VOS}_3 = \text{VOS}_2 + \{9s, 8p, 7d, 6f, 7g\},$$

$$\text{VOS}_4 = \text{VOS}_3 + \{10s, 9p, 8d, 7f, 8g\},$$

$$\text{VOS}_5 = \text{VOS}_4 + \{11s, 10p, 9d, 8f, 9g\}.$$

The core was opened for SRD substitutions step by step. For the VOS_1 one core shell $5s$ was opened for SD excitations; for the next VOS_2 all $n = 4$ shells were opened for SRD substitution. For VOS_5 all core shells were opened. In the VOS_5 the number of CSFs was 67 325 for odd-parity and 32 049 for even-parity configurations. For each VOS the number of optimized levels for odd parity was extended by 5 and in the end (VOS_5) it reached 27. This included levels $5p^5 ns^{1,3}P$, $n = 6$–11; and $5p^5 nd^{1,3}P$ and $5p^5 nd^3D$, $n = 5$–9.
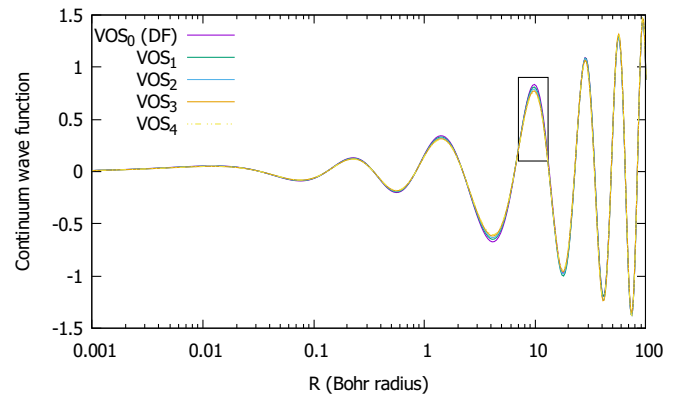

FIG. 1. Large components of the normalized continuum orbitals with $J = -1/2$ and $\kappa = -1$ for different ionic virtual sets. The kinetic energy of the continuum electron is equal to 0.0007 hartree. The fragment marked with a box is enlarged in Fig. 2.
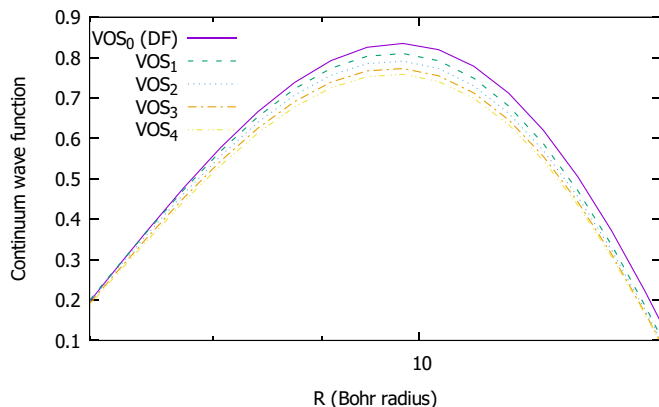
FIG. 2. Same as in Fig. 1, but for a smaller R-axis range. Small differences for different complexes are shown, but the convergence of the results with an increasing number of CSFs is clearly visible.

B. The Xe$^+$ ion

The active set for the states $[Kr]4d^{10}5s^25p^5\,^2P_{1/2,3/2}$ was generated in the same manner as for the Xe atom. The wave functions of Xe$^+$ were taken from the atom ground state $[Kr]4d^{10}5s^25p^6\,^1S_0$ and the mixing coefficients were obtained by the relativistic configuration interaction computation.

VI. CONTRIBUTION OF BOUND STATES TO THE EDM

The atomic states for EDM calculations were built from electronic orbitals optimized separately for each state. In general, this approach results in electronic orbitals, which are considered optimal for the calculations of matrix elements of the EDM operators, but they are not necessarily optimal for calculations of transition energies [27]. Therefore, we applied a strategy where the EDM matrix elements were calculated *ab initio* from separately optimized atomic states, while the transition energies were adopted from the NIST database [28].

Data for the EDM for ^{129}Xe from the TPT, PSS, NSM, and eEDM interactions, presented in Table I, are only from the ground state and were computed by Eq. (8). All EDM values computed with the NIST energies, except those from DF interactions, are larger than values calculated with the GRASP2K energies.

To estimate the EDM contribution from the Rydberg states of ^{129}Xe, the Riemann ζ tail procedure described in [18] was applied. The main goal of this procedure was to evaluate the upper bound of the infinite tail of the sum (8), which contains the contribution to the EDM from Rydberg states. This contribution, divided by sum of the five leading terms in (8), was found to be 1.5%.

VII. COMPUTATIONS OF CONTINUUM WAVE FUNCTIONS FOR THE Xe$^+ + e^-$ SYSTEM

Wave functions of the continuum states were generated in the ionic field described in Sec. V B. The results of Xe$^+$ energies calculated with different virtual sets are collected in Table II. As expected, the differences between consecutive energies become smaller along with the growing size of the active space used. These virtual sets were used further in the generation of continuum orbitals.

The kinetic energies of the continuum electron used in our calculations cover the range of 0.0001–10.0 hartree. They were chosen as 0.0001, 0.0003, 0.0005, 0.0007, 0.0009, 0.001, 0.003, 0.005, 0.007, 0.009, 0.01, 0.03, 0.05, 0.07, 0.1, 0.2, 0.3, 0.4, 0.5, 0.7, 1.0, 1.5, 2.0, 5.0, and 10.0 hartree. Here only the s wave ($\kappa = -1$) was calculated, since only this one was used in further EDM calculations. The continuum orbital wave functions were calculated on a relatively extensive grid, e.g., 90 000 points were used on the asymptotically linear exponential grid (which correspond to $R_{\max} = 397\,538$ and 1258 bohrs for the lowest and highest energies from the list, respectively). Such long grids were required to find the accurate amplitude of the wave function needed for normalization.

Large components of the continuum orbitals of the continuum wave functions for a selected energy are presented in Figs. 1 and 2. The amplitude becomes slightly smaller with enlargement of the virtual sets.

VIII. COMPUTATIONAL ACCURACY OF THE CONTINUUM WAVE FUNCTIONS

The continuum orbitals were calculated with the modified version of the COWF code, which was originally prepared in frames of the RATIP package. The modifications have adapted the code to the newest version of the GRASP2K package.

To ensure that the modified code correctly generates continuum wave functions, two tests were performed. In the first

TABLE III. Calculated phase shifts for the Xe $+ e^-$ system with the different numbers of CSFs used (N_{CSF}), compared to the previous computations [23].

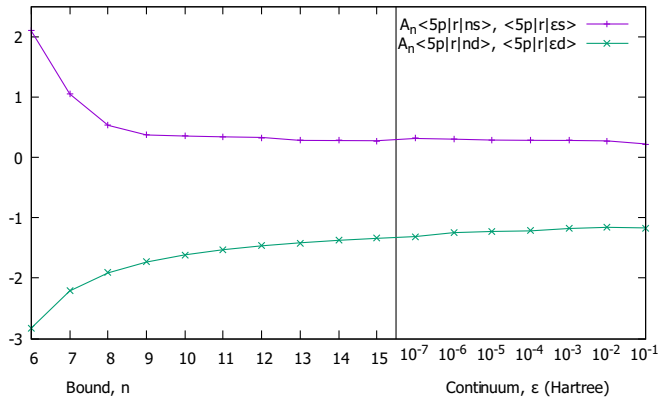|		Ref. [23]		Present work		
ϵ (eV)	κ	$N_{\text{CSF}} = 1$	$N_{\text{CSF}} = 827$	$N_{\text{CSF}} = 3$	$N_{\text{CSF}} = 137$	$N_{\text{CSF}} = 2337$
10	-1	1.452	1.448	1.451	1.446	1.444
10	1	-1.074	-1.070	-1.076	-1.075	-1.073
10	-2	-1.170	-1.169	-1.166	-1.173	-1.170
10	2	0.995	0.975	0.984	0.971	0.962
10	-3	0.982	0.975	0.971	0.958	0.952
10	3	0.111	0.110	0.109	0.109	0.109
10	-4	0.115	0.114	0.113	0.113	0.113

FIG. 3. Continuity across the series limit $\epsilon = 0$ for the electric dipole radial integrals. To the left of the vertical line are calculated radial integrals for the Rydberg states (where $A_n = \sqrt{n^3/2}$) and to the right for the continuum states.

FIG. 4. Dependence of eEDM values for all interactions of the continuum energy, for the p^- orbital in the VOS$_2$ approximation. The ground-state configuration for Xe$^+$ is $J = 3/2, 1/2$ with fitted equations.

test, scattering phase shifts were calculated for elastic scattering of electrons from ^{129}Xe. Calculations were performed for three virtual orbital sets of $J = 0$ and the results were compared to the results from [23] (see Table III). None of the calculations accounted for correlation effects. This test was repeated for different energies and higher partial waves of the continuum electron, and also for the case of $J = 1$. In all cases the results from [23] were reproduced correctly.

In the second test, electric dipole radial integrals $A_n \langle 5p|r|ns \rangle$ and $A_n \langle 5p|r|nd \rangle$ ($A_n = \sqrt{n^3/2}$, $n = 6, \ldots, 15$) were calculated involving the outer electron in the Rydberg series $5s^2 5p^5 ns$ and $5s^2 5p^5 nd$. They were matched to integrals $\langle 5p|r|\epsilon s \rangle$ and $\langle 5p|r|\epsilon d \rangle$, calculated for the continuum orbitals $P_{\kappa\epsilon}$ and $Q_{\kappa\epsilon}$, for a set of energies ϵ from 10^{-7} up to 10^{-1} hartree. The results are presented in Fig. 3. It is clearly shown that continuity through the ionization limit was achieved.

Although in the EDM calculations only the s wave ($\kappa = -1$) was considered, the above tests were also performed for higher values of κ. This way it has been shown that the continuum orbitals were calculated and normalized correctly.

IX. THE EDM RESULTS FROM THE CONTINUUM STATES

Using the wave functions of the continuum electron, we computed the matrix elements between ground and continuum-state functions of the Xe atom, namely, $\langle 0|\hat{D}_z|c \rangle$ and $\langle c|\hat{H}_{\text{int}}|0 \rangle$, and then computed the EDM contributions in VOS$_2$ for each state from the continuum. These values of the eEDM for $J = 3/2, 1/2$ for p^- are plotted in Fig. 4 as an example. The fitting procedure allows us to obtain the dependence of EDM values for all interactions from energies of the continuum states. We found the best-fitting function

$$f^{\text{int}}(E_c) = \frac{-A}{(1 + aE_c)^{1/b}}. \tag{15}$$

It should be mentioned that the parameters a and b were matched in the second decimal place for the same VOS, J, and p orbital. After integration of these functions according to the formula (9), the EDM contributions from the continuum states were obtained.
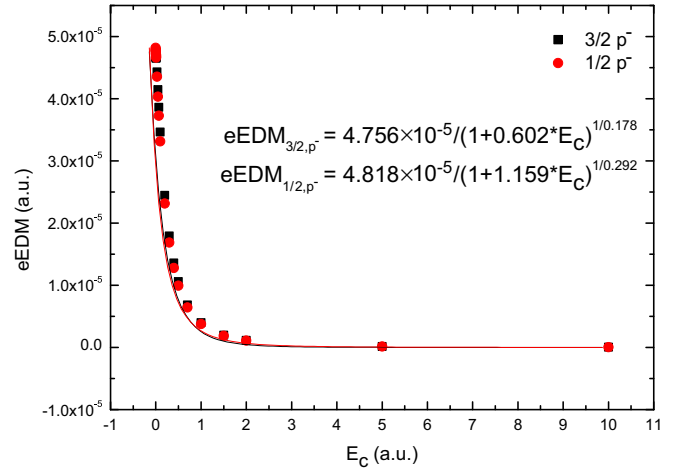
The contribution of the continuum states for all interaction was computed in VOS$_2$ and is presented in Table IV. All these contributions were computed with the experimental ionization limit from the NIST database [28]: 0.445 763 535 4 for Xe II $5s^2 5p^5$ $^2P^o_{3/2}$ and 0.493 773 699 49 for $5s^2 5p^5$ $^2P^o_{1/2}$ (both values in a.u.). The theoretical ionization limits, computed with the total energies from the MCDHF method for atoms and ions, are 0.562 291 606 and 0.598 999 075 (in a.u.), respectively. The contributions computed with experimental values of ionization limits are slightly bigger than those obtained with the MCDHF method. In Table IV the sum of all states in the continuum is also presented (see the last column).

A summary of the computations is presented in Table V. Also the sum of contributions to the EDM from bound and

TABLE IV. Individual continuum states and the sum of their contributions to the interactions. The TPT (in $10^{-20} C_T \langle \sigma_N \rangle |e|$ cm), PSS (in $10^{-20} C_T \langle \sigma_A \rangle |e|$ cm), NSM (in $10^{-17} [S/(|e| \text{ fm}^3)]|e|$ cm), and eEDM (in $d_e \times 10^{-4}$) interaction contributions to the EDM are calculated in VOS$_2$ for ^{129}Xe. Here Th and Ex indicate the results obtained with the excitation energy taken from GRASP2K and the NIST database [28], respectively.

	$J = 3/2$		$J = 1/2$		
	p^-	p^+	p^-	p^+	Σ
		TPT			
Th	0.17	-0.84×10^{-4}	0.07	-0.86×10^{-4}	0.24
Ex	0.08	-0.98×10^{-4}	0.08	-0.97×10^{-4}	0.16
		PSS			
Th	0.20	0.01	0.20	0.01	0.42
Ex	0.23	0.01	0.23	0.01	0.48
		NSM			
Th	0.02	0.03	0.02	0.03	0.10
Ex	0.02	0.03	0.02	0.03	0.10
		eEDM			
Th	0.31	-0.14	0.30	-0.14	0.33
Ex	0.34	-0.16	0.34	-0.16	0.36

TABLE V. The TPT (in $10^{-20}C_T\langle\sigma_N\rangle|e|$ cm), PSS (in $10^{-20}C_T\langle\sigma_A\rangle|e|$ cm), NSM (in $10^{-17}[S/(|e|\,\text{fm}^3)]|e|$ cm), and eEDM (in $d_e \times 10^{-4}$) interaction contributions to the EDM from bound and continuum states, for the ground state of ^{129}Xe, compared with data from other methods. Here Th and Ex indicate the results obtained with the excitation energy taken from GRASP2K and the NIST database [28], respectively.

	TPT		PSS		NSM		eEDM	
	Th	Ex	Th	Ex	Th	Ex	Th	Ex
bound states	0.16	0.33	0.45	0.95	0.09	0.20	0.24	0.54
CS	0.24	0.16	0.42	0.48	0.10	0.10	0.33	0.36
Σ	0.40	0.49	0.87	1.43	0.19	0.30	0.57	0.90
DHF[a]		0.45		1.3		0.29		0.85
RPA[a]		0.57		1.6		0.38		1.00
DHF[b]		0.41						
RPA[b]		0.52						
DHF[c]		0.41						
RPA[d]						0.38		
DHF[e]								0.86
RPA[e]								1.05
DF[f]		0.45				0.29		
MBPT[f]		0.41				0.27		
MBPT[f]		0.52				0.34		
CPHF[f]		0.56				0.38		
CC[f]		0.61				0.42		
CC[f]		0.50				0.34		
CC[f]		0.50				0.34		
CPHF[g]		0.56						

[a]Reference [10].
[b]Reference [29].
[c]Reference [30].
[d]Reference [31].
[e]Reference [32].
[f]Reference [32].
[g]Reference [12].

continuum states according Eq. (7) is presented. Let us stress here that the values from the CS are of the same order as those computed from the bound states.

X. UNCERTAINTY ESTIMATES

Since the present work is based on *ab initio* calculations, it is not easy to estimate the overall uncertainty.

However, the possible sources of uncertainties may be identified.

Two of these error sources are electron correlation effects and wave-function relaxation. Their contributions to the overall error budget can be estimated by comparing the EDM results for bound states, obtained for different virtual orbital sets DF–VOS$_5$. By comparing the last two rows in Table I, we can estimate this contribution as approximately 5%.

In the present work only SRD substitutions were used to generate virtual orbital sets, thus the double (partially), triple, and higher-order substitutions were omitted. In general, this might affect the result around 10%–20%, but it is often partly canceled and usually remains below 10% [33]. In the case of Xe, we estimate this contribution as 5%.

The correlation term in Eq. (3) is omitted. In the case of xenon this may affect the CS wave function by approximately 5%. This is based on the calculations with and without a correlation term in [23].

Our neglect of the QED effects and Breit interaction also contributes to the total error budget. It is estimated as 1%.

In Eqs. (9) and (10) numerical methods are employed for fitting and integrating. We estimate the fitting error as no more than 2%. Since the integrand is a smooth function, the integrating error is estimated to be less than 1%.

Taking all of the above contributions into account, we estimate the relative standard error of the mean $\sigma_{\bar{x}} = 20\%$.

XI. CONCLUSION

The method for generating continuum electron wave functions in the framework of the MCDHF method were presented in the context of the EDM for many-electron atoms. The continuity across the ionization energy of radial integrals involving the Rydberg and continuum states was ensured. As an example, the contributions to the atomic EDM of ^{129}Xe, from both discrete and continuum states, were estimated using the MCDHF method. We showed that the contribution of the continuum electron to the atomic EDM is comparable in size to the contribution of the bound states. Therefore, in the accurate calculations of EDMs it is necessary to evaluate the continuum contribution.

ACKNOWLEDGMENTS

[1] I. B. Khriplovich and S. K. Lamoreaux, *CP Violation Without Strangeness* (Springer, Berlin, 1997).

[2] K. Jungmann, Ann. Phys. (Berlin) **525**, 550 (2013).

[3] V. A. Dzuba, V. V. Flambaum, and C. Harabati, Phys. Rev. A **84**, 052108 (2011).

[4] Y. Singh and B. K. Sahoo, Phys. Rev. A **91**, 030501 (2015).

[5] T. Chupp and M. Ramsey-Musolf, Phys. Rev. C **91**, 035502 (2015).

[6] T. Inouea, T. Furukawaa, T. Nanaoa, A. Yoshimib, K. Suzukia, M. Chikamoria, M. Tsuchiyaa, H. Hayashia, M. Uchidaa, and K. Asahia, Phys. Proc. **17**, 100 (2011).

[7] T. Furukawa, T. Inoue, T. Nanao, A. Yoshimi, M. Tsuchiya, H. Hayashi, M. Uchida, and K. Asahi, J. Phys.: Conf. Ser. **312**, 102005 (2011).

[8] F. Kuchler *et al.*, Hyperfine Interact. **237**, 95 (2016).

[9] M. A. Rosenberry and T. E. Chupp, Phys. Rev. Lett. **86**, 22 (2001).

[10] V. A. Dzuba, V. V. Flambaum, and S. G. Porsev, Phys. Rev. A **80**, 032120 (2009).

[11] Y. Singh, B. K. Sahoo, and B. P. Das, Phys. Rev. A **89**, 030502(R) (2014).

[12] K. V. P. Latha and P. R. Amjith, Phys. Rev. A **87**, 022509 (2013).

[13] S. G. Porsev, M. S. Safronova, and M. G. Kozlov, Phys. Rev. Lett. **108**, 173001 (2012).

[14] V. G. Gorshkov, V. F. Ezhov, M. G. Kozlov, and A. I. Mikhailov, Sov. J. Nucl. Phys. **48**, 867 (1988).

[15] P. Jönsson, G. Gaigalas, J. Bieroń, C. Froese Fischer, and I. Grant, Comput. Phys. Commun. **184**, 2197 (2013).

[16] P. Syty and S. Fritzsche (private communication).

[17] S. Fritzsche, Comput. Phys. Commun. **183**, 1525 (2012).

[18] L. Radžiūtė, G. Gaigalas, P. Jönsson, and J. Bieroń, Phys. Rev. A **90**, 012528 (2014).

[19] G. Gaigalas, T. Zalandauskas, and Z. Rudzikas, At. Data Nucl. Data Tables **84**, 99 (2003).

[20] G. Gaigalas, T. Zalandauskas, and S. Fritzsche, Comput. Phys. Commun. **157**, 239 (2004).

[21] H. Saha, Phys. Rev. A **43**, 4712 (1991).

[22] I. P. Grant, B. J. McKenzie, P. H. Norrington, D. F. Mayers, and N. Pyper, Comput. Phys. Commun. **21**, 207 (1980).

[23] P. Syty, J. E. Sienkiewicz, and S. Fritzsche, Rad. Phys. Chem. **68**, 301 (2003).

[24] P. Burke, A. Hibbert, and W. Robb, J. Phys. B **4**, 153 (1971).

[25] R. D. Cowan, *The Theory of Atomic Structure and Spectra* (University of California Press, Oakland, 1981), pp. 522–524.

[26] K. G. Dyall, I. P. Grant, C. T. Johnson, F. A. Parpia, and E. P. Plummer, Comput. Phys. Commun. **55**, 425 (1989).

[27] J. Bieroń, G. Gaigalas, E. Gaidamauskas, S. Fritzsche, P. Indelicato, and P. Jönsson, Phys. Rev. A **80**, 012513 (2009).

[28] A. Kramida, Y. Ralchenko, J. Reader, and NIST ASD Team, NIST atomic spectra database, version 5.5.6, available at https://physics.nist.gov/asd (National Institute of Standards and Technology, Gaithersburg, 2018).

[29] A.-M. Mårtensson-Pendrill, Phys. Rev. Lett. **54**, 1153 (1985).

[30] V. A. Dzuba, V. V. Flambaum, and P. G. Silvestrov, Phys. Lett. **154B**, 93 (1985).

[31] V. A. Dzuba, V. V. Flambaum, J. S. M. Ginges, and M. G. Kozlov, Phys. Rev. A **66**, 012111 (2002).

[32] A.-M. Mårtensson-Pendrill and P. Öster, Phys. Scr. **36**, 444 (1987).

[33] J. Bieroń, C. Froese Fischer, P. Jönsson, and P. Pyykkö, J. Phys. B **41**, 115002 (2008).